



# Whipple shield performance in the shatter regime

S. Ryan<sup>a,\*</sup>, M. Bjorkman<sup>b</sup>, E.L. Christiansen<sup>c</sup>

<sup>a</sup>USRA Lunar and Planetary Institute, 3600 Bay Area Blvd, Houston, TX 77058, USA

<sup>b</sup>Jacobs Engineering, 2224 Bay Area Blvd, Houston, TX 77058, USA

<sup>c</sup>NASA Johnson Space Center, 2101 NASA Pkwy, Houston, TX 77058, USA

## ARTICLE INFO

### Article history:

Available online 26 January 2011

### Keywords:

Hypervelocity impact  
Orbital debris  
Whipple shield  
Ballistic limit

## ABSTRACT

A series of hypervelocity impact tests have been performed on aluminum alloy Whipple shields to investigate failure mechanisms and performance limits in the shatter regime. Test results demonstrated a more rapid increase in performance than predicted by the latest iteration of the JSC Whipple shield ballistic limit equation (BLE) following the onset of projectile fragmentation. This increase in performance was found to level out between 4.0 and 5.0 km/s, with a subsequent decrease in performance for velocities up to 5.6 km/s. For a detached spall failure criterion, the failure limit was found to continually decrease up to a velocity of 7.0 km/s, substantially varying from the BLE, while for perforation-based failure an increase in performance was observed. An existing phenomenological ballistic limit curve was found to provide a more accurate reproduction of shield behavior than the BLE, prompting an investigation of appropriate models to replace linear interpolation in shatter regime. A largest fragment relationship was shown to provide accurate predictions up to 4.3 km/s, which was extended to the incipient melt limit (5.6 km/s) based on an assumption of no additional fragmentation. Alternate models, including a shock enhancement approach and debris cloud cratering model are discussed as feasible alternatives to the proposed curve in the shatter regime, due to conflicting assumptions and difficulties in extrapolating the current approach to oblique impact. These alternate models require further investigation.

© 2010 Published by Elsevier Ltd.

## 1. Introduction

In 1947 Fred Whipple suggested that a thin “bumper”, when placed in front of the pressure hull of a space vehicle, would substantially increase the vehicle’s level of protection against impacting meteors. From Apollo through to the International Space Station, the Whipple shield concept has provided the baseline for shielding against the impact of micrometeoroids and orbital debris (MMOD). Over the range of impact velocities relevant for Earth-orbiting spacecraft, the performance of a Whipple shield is characterized in three parts: low velocity, shatter, and hypervelocity. In the low velocity regime, the projectile perforates the shield bumper plate, and propagates to the rear wall, intact (albeit possibly deformed and eroded). Transition to the shatter regime occurs once the impact shock amplitudes are sufficient to induce fragmentation of the projectile. Within the shatter regime, further increases in projectile velocity result in increased projectile fragmentation, transitioning from a small number of solid fragments to a multitude of small, finely dispersed mixed phase debris cloud (solid and molten fragments). Transition to the hypervelocity regime is defined by the point at which the rear wall failure mechanism

changes from cratering-based to impulsive, similar to that induced by a blast wave. Increased impact speeds within the hypervelocity regime are expected to increase the debris cloud kinetic energy, resulting in a decrease in shielding performance.

Ballistic limit equations (BLEs) are used to design and evaluate the performance of shields for MMOD protection. For a metallic Whipple shield, the new non-optimum equation (NNO) [1], or variations thereof (e.g. [2]) are commonly used. These equations are based on cratering relationships in the low velocity regime, kinetic energy scaling in the hypervelocity regime, and a linear interpolation between the two in the shatter regime. With a debris environment increasingly dominated by manmade debris, vehicles operating in low earth orbit (LEO) are subjected to slower median encounter velocities. As such, the performance of shielding at velocities in the shatter regime is increasingly important to mission risk predictions. In this paper, the results of an experimental impact study to characterize failure limits of an aluminum alloy Whipple shield in the shatter regime are presented.

## 2. Predicting the failure limit of metallic Whipple shields

For this analysis, a recent iteration of the Whipple shield ballistic limit equation, referred to herein as the JSC Whipple shield equation, is used. This equation is based on the NNO approach and

\* Corresponding author. Tel.: +61 (0)3 96267706; fax: +61 (0)3 96268999.  
E-mail address: [shannon.ryan@dsto.defence.gov.au](mailto:shannon.ryan@dsto.defence.gov.au) (S. Ryan).

**Nomenclature**

$d$	diameter (cm)
$S$	shield spacing (cm)
$t$	thickness (cm)
$V$	velocity (km/s)
$\theta$	impact angle (deg)
$\rho$	density (g/cm <sup>3</sup> )
$\sigma$	yield strength (MPa)

**Subscripts**

$b$	bumper
$c$	critical
$f$	fragment
$n$	normal
$p$	projectile
$w$	rear wall

incorporates a selection of modifications proposed by Reimerdes et al. [2], namely the de-rating of shield performance ( $F_2^*$ ) in the hypervelocity regime for bumpers that are insufficiently thick to effectively fragment the projectile. Proposed modifications to the low velocity regime limit velocity,  $V_{LV}$ , based on bumper thickness to projectile diameter ratio from [2] are also incorporated, albeit in the original form proposed in [3]. The JSC Whipple shield ballistic limit equation is defined as:

In the low velocity regime, i.e.  $V_n \leq V_{LV}$ :

$$d_c = \left[ \frac{t_w(\sigma/40)^{1/2} + t_b}{0.6(\cos\theta)^{5/3} \rho_p^{1/2} V^{2/3}} \right]^{18/19} \quad (1)$$

where  $V_{LV} = 2.60$  if  $t_b/d_p \geq 0.16$  and  $1.436 \times (t_b/d_p)$  if  $t_b/d_p < 0.16$

In the hypervelocity regime, i.e.:  $V_n \geq 7$  km/s:

$$d_c = 3.918 F_2^* \frac{t_w^{2/3} S^{1/3} (\sigma/70)^{1/3}}{\rho_p^{1/3} \rho_b^{1/9} (V \cos \theta)^{2/3}} \quad (2)$$

In the shatter regime, i.e.  $V_{LV} < V_n < 7$  km/s, linear interpolation is applied:

$$d_c = d_c(V_{LV}) + \frac{(d_c(V_{HV}) - d_c(V_{LV}))}{V_{HV} - V_{LV}} \times (V_n - V_{LV}) \quad (3)$$

The de-rating factor,  $F_2^*$ , is calculated as:

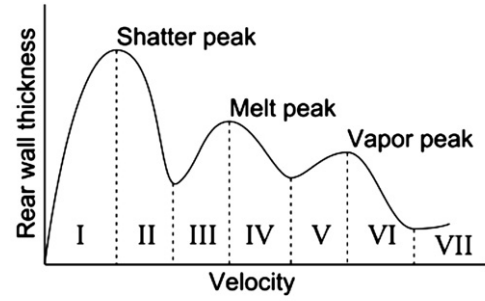
$$F_2^* = \begin{cases} 1 & \text{for } (t_b/d_p) \geq (t_b/d_p)_c \\ r_{S/D} - 2 \frac{(t_b/d_p)}{(t_b/d_p)_c} (r_{S/D} - 1) + \left( \frac{(t_b/d_p)}{(t_b/d_p)_c} \right)^2 (r_{S/D} - 1) & \text{for } (t_b/d_p) < (t_b/d_p)_c \end{cases} \quad (4)$$

where,

$$(t_b/d_p)_c = \begin{cases} 0.2(\rho_p/\rho_b) & \text{for } S/d_p \geq 30 \\ 0.25(\rho_p/\rho_b) & \text{for } S/d_p < 30 \end{cases} \quad (5)$$

and  $r_{S/D}$  is ratio between the required rear wall thickness when the bumper thickness is zero, and when it is equal to the limit  $(t_b/d_p)_c$ , i.e.:

$$r_{S/D} = \frac{t_w(t_b = 0)}{t_w(t_b/d_p = (t_b/d_p)_c)} = \frac{(0.6 \cdot d_p^{19/18} (\cos\theta)^{5/3} \rho_p^{1/2} V_{HV}^{2/3} - t_b) / (\sigma/40)^{1/2}}{(d_p/3.918 \cdot \rho_p^{-1/3} \rho_b^{-1/9} (V_{HV} \cos\theta)^{-2/3} S^{1/3} (\sigma/70)^{1/3})^{3/2}} \quad (6)$$



Phenomenological curve velocity limits	
Region I	$V < 3.1$ km/s
Region II	$3.1 < V < 4.3$ km/s
Region III	$4.3 < V < 5.6$ km/s
Region IV	$5.6 < V < 7.0$ km/s
Region V, VI, VIII	$V > 7.0$ km/s

Fig. 1. Phenomenological ballistic limit curve for an Al-alloy Whipple shield (reproduced from [5]) with velocity limits.

Although providing a reasonable and conservative simplification of shield performance for risk assessment, the linear interpolation in the shatter regime may not accurately reproduce the actual behavior observed for this shield type. In 1970, Swift et al. [4] reported on a series of hypervelocity impact experiments that were performed on aluminum shields with constant spacing and bumper thickness, while the shield rear wall thickness was varied in order to determine the failure threshold. To effectively describe the types of damage observed in target photographs, and in an effort to better characterize the impact performance of a dual-wall structure, Hopkins et al. [5] defined a phenomenological ballistic limit curve (BLC), shown in Fig. 1. The authors defined the characteristics of each region based on their observation of rear wall damage, summarized as follows. In region I, the typical damage observed was a single crater – indicating an intact projectile. In region II, typical damage graduated from a few fairly large craters to a multitude of small craters as a result of the onset and escalation of projectile fragmentation. In region III, the appearance of damage remained rather constant, with each individual crater increasing in size and depth. In region IV, solid fragment craters similar in appearance to those in region II/III were increasingly interspersed by soft contour craters made by molten fragments. Throughout region V, soft contour craters caused by molten material were the dominant damage observable. Region VI damage was characterized by a mixture of molten and vapor damage, where the

failure transitions from penetration and perforation to rupture and tearing at the upper velocity limits. Damage in region VII was similar to that of pressing by high-pressure gas.

### 3. Impact testing

A total of 82 hypervelocity impact tests were performed with spherical Al2017-T4 projectiles on aluminum alloy Whipple shields nominally identical to those tested by Swift et al. [4]. The thickness of the Al6061-T6 bumper ( $t_b = 0.079$  cm), shield spacing ( $S = 5.08$  cm) and projectile diameter ( $d_p = 0.3175$  cm) were constant, while the Al6061-T6 rear wall thickness ( $t_w$ ) was varied to determine the shield failure limits. Tests were performed at varying impact angles ( $0^\circ/45^\circ/60^\circ$ ) and over a range of velocities

Download English Version:

<https://daneshyari.com/en/article/778631>

Download Persian Version:

<https://daneshyari.com/article/778631>

[Daneshyari.com](https://daneshyari.com)